

We extend the saturation models *à la* Golec-Biernat and Wüsthoff to cross-sections of hard processes initiated by virtual-gluon probes separated by large rapidity intervals at hadron colliders. We derive their analytic expressions and apply them to physical examples, such as saturation effects for Mueller-Navelet jets. By comparison to $\gamma^* - \gamma^*$ cross-sections we find a more abrupt transition to saturation. We propose to study observables with a potentially clear saturation signal and to use heavy vector and flavored mesons as alternative virtual-gluon probes.

I. INTRODUCTION

The saturation regime describes the expected high-density phase of partons in QCD. It may occur for instance when the Balitsky-Fadin-Kuraev-Lipatov (BFKL) QCD evolution equation[1] goes beyond some energy limit[2, 3, 4, 5, 6, 7]. On a phenomenological ground, a well-known saturation model[8] by Golec-Biernat and Wüsthoff (GBW) gives an interesting parametrisation of the proton structure functions in the HERA energy range. It provides a simple and elegant formulation of the transition to saturation. However, there does not yet exist a clear confirmation of saturation since the same data can well be explained within the conventional perturbative QCD framework[9].

An interesting question is whether the experiments at high-energy hadron colliders, such as the Tevatron or LHC, can test saturation, while for the moment this search is mainly considered for heavy-ion collisions. In the present paper, our aim is to look for saturation effects in the context of hadron-induced hard collisions. The key difference with electron-induced reactions is that the hard probe is no more a virtual photon γ^* but mainly a virtual gluon g^* , see Fig.1a.

A basic ingredient of saturation models is the QCD dipole formalism[10, 11]. Let us then introduce the general dipole formulation of hard total cross-sections. It reads

$$\sigma = \int d^2r_1 dz_1 d^2r_2 dz_2 \phi^{(1)}(r_1, z_1, Q_1^2) \phi^{(2)}(r_2, z_2, Q_2^2) \sigma_{dd}(\Delta\eta, r_1, r_2, z_1, z_2), \quad (1)$$

where $r_{i=1,2}$ are the transverse sizes of the dipoles, $z_{i=1,2}$ the fraction of longitudinal momentum of the quarks in each dipole, and $\Delta\eta$ is the pseudo-rapidity range¹ of the dipole-dipole cross-section $\sigma_{dd}(\Delta\eta, r_1, r_2, z_1, z_2)$, see Fig.1b. In our notations, $\phi^{(i)}(r_i, z_i, Q_i^2)$ are the dipole distributions in the target and projectile, and Q_i the virtuality of the hard probes.

The k_T -factorization property [12] provides the general formalism for coupling external sources to the BFKL kernel, through the convolution of *impact factors*. It can be proved that k_T -factorization is equivalent[13] to the factorization of the dipole distributions $\phi^{(i)}(r_i, z_i, Q_i^2)$ expressed by formula (1). These dipole distributions can thus be derived from the corresponding *impact factors*. In the γ^* case, the dipole distribution functions $\phi^\gamma(r, z, Q^2)$ are the known QED wave functions squared[14], of a virtual photon into $q\bar{q}$ states. In the g^* case[15, 16], the same equivalence allows one to define a dipole distribution $\phi^g(r, z, Q^2)$. In the present paper, we will make the simplifying assumption that the k_T -factorization property is preserved in the presence of saturation (see a recent discussion in [17]).

In this context, we may formulate the GBW saturation model for hadron collisions. Initially, the GBW approach[8] is a model for the dipole-proton cross-section which includes the saturation damping of large-dipole configurations. For the description of $\gamma^* - \gamma^*$ cross-sections at LEP, see Ref.[18], it has been extended² to dipole-dipole cross-sections. The same saturation scale is considered for dipole-dipole and dipole-proton cross-sections. The parametrisation of this dipole-dipole cross-section is

$$\sigma_{dd} = \sigma_0 \left\{ 1 - \exp \left(- \frac{r_{\text{eff}}^2}{4R_0^2(\Delta\eta)} \right) \right\}, \quad (2)$$

‡ URA 2306, unité de recherche associée au CNRS.

*Electronic address: marquet@spht.saclay.cea.fr

†Electronic address: pesch@spht.saclay.cea.fr

¹ More precisely it is defined by the smaller rapidity distance between the q or \bar{q} constituents of the top and bottom dipoles[11].

² For our purpose, we shall only use a high-energy approximation of the expressions quoted by the authors[18].

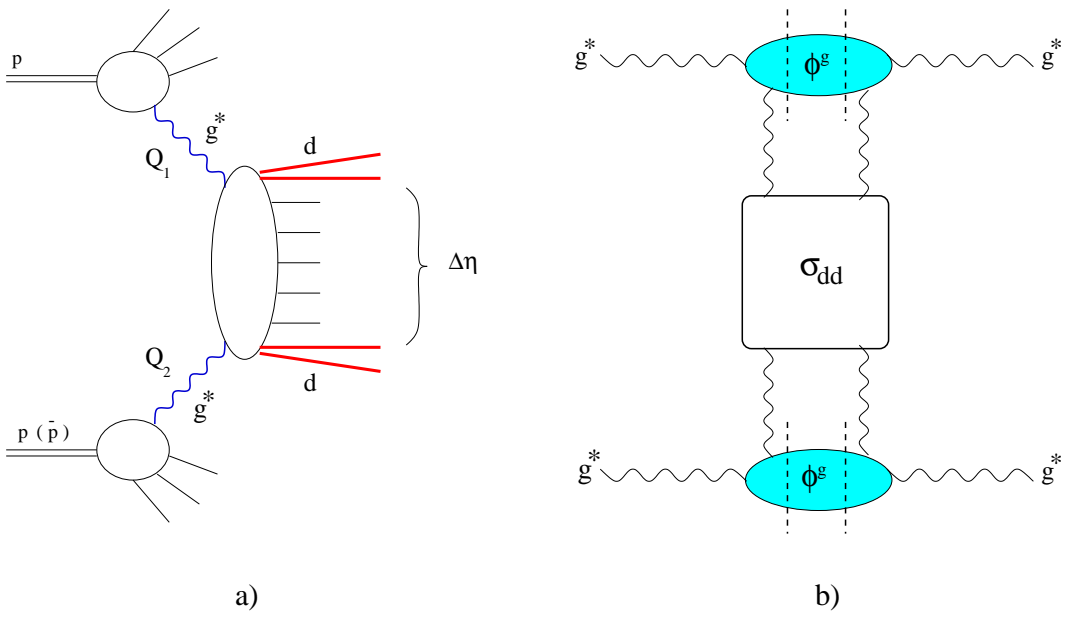


FIG. 1: *Hard high-energy cross-sections at hadron colliders.* Fig 1a: hard dipole-dipole production at hadron colliders. $\Delta\eta$: rapidity gap between the two hadronic probes. $Q_{1,2}$: virtualities of the gluons that initiate the reaction. Fig 1b: g^*-g^* total cross-sections. ϕ^g : virtual gluon dipole distribution. σ_{dd} : the dipole-dipole cross-section. Dashed line: intermediate color-singlet $q\bar{q}$ dipole state (see text).

where $R_0(\Delta\eta)$ is the rapidity-dependent saturation radius and the dipole-dipole *effective* radius $r_{\text{eff}}^2(r_1, r_2)$ is defined[18] in such a way to satisfy *color transparency*, namely $\sigma_{dd} \propto r_{i=1,2}^2$ when $r_i \rightarrow 0$. In the present paper, we extend further the GBW model by taking into account saturation for g^* -induced hard cross-sections.

The plan of the paper is as follows. In section II, we recall the ingredients of our approach, namely the dipole distributions for hard probes and the extension of the GBW model to dipole-dipole cross-sections. In section III, we derive our results for the hard cross-sections with saturation. In section IV, we discuss these results in the prospect of experiments at the Tevatron and LHC and propose characteristic observables, suitable for testing saturation. The final section V is devoted to conclusion and outlook.

II. FORMULATION

Let us first recall how one can derive dipole distributions associated with an initial virtual gluon g^* . Using k_T -factorization properties, it is possible to derive the dipole distribution $\phi^g(r, z, Q^2)$ in the BFKL framework[15, 16]. The virtual gluon initiating the hard process corresponds to a transverse³ gluon of virtuality Q being at the end of a Dokshitzer-Gribov-Lipatov-Altarelli-Parisi (DGLAP) gluon ladder[9]. One obtains[15],

$$\phi^g(r, z, Q^2) = \left(z^2 + (1-z)^2 \right) \hat{Q}^2 \frac{5}{2\pi} {}_2F_3 \left(\frac{7}{2}, 3; 4, 2, 2, -v^2 \right), \quad (3)$$

where $v \equiv r\hat{Q} \equiv rQ\sqrt{z(1-z)}$ and ${}_2F_3$ is a hypergeometric function[19]. Formula (3) is to be compared with the virtual (transverse) photon distribution

$$\phi^\gamma(r, z, Q^2) \propto \left(z^2 + (1-z)^2 \right) \hat{Q}^2 K_1^2(v), \quad (4)$$

³ The longitudinal component is not present at leading order[9].

where K_1 is the modified Bessel function of the second kind. Since the GBW cross-sections (2) are z -independent, we only have to consider the distributions ϕ integrated over z . For the integrated function ϕ^g , one simply obtains

$$\phi^g(r, Q^2) \equiv \int_0^1 dz \phi^g(r, z, Q^2) = \frac{Q}{2\pi r} J_1(Qr) , \quad (5)$$

where J_1 is the Bessel function.

A theoretical comment is in order. *Via* its equivalence to dipole factorization at leading-log level, k_T -factorization leads to a description of a virtual gluon in terms of colorless $q\bar{q}$ dipoles. This means that the color quantum number carried by the *incoming* virtual gluon g^* flows into an *outgoing* soft gluon participating to the BFKL ladder, see Fig.1b, and that other possible color configurations do not contribute within this approximation. We assume this configuration to be also valid when the transition to saturation occurs. This, of course, will need further theoretical investigation[17]. Note that contrary to the photon, the factorized dipole distribution for the virtual gluon is not positive-definite and therefore cannot be interpreted as a probability distribution. We will come back to this point later on.

Concerning the application[18] of the GBW model to the dipole-dipole cross-sections, see formula (2), three scenarios for $r_{\text{eff}}(r_1, r_2)$ are considered:

$$\begin{aligned} \mathbf{1.} \quad r_{\text{eff}}^2 &= \frac{r_1^2 r_2^2}{r_1^2 + r_2^2} , \\ \mathbf{2.} \quad r_{\text{eff}}^2 &= \min(r_1^2, r_2^2) , \\ \mathbf{3.} \quad r_{\text{eff}}^2 &= \min(r_1^2, r_2^2) \{1 + \ln(\max(r_1, r_2)/\min(r_1, r_2))\} . \end{aligned} \quad (6)$$

All three parametrisations exhibit *color transparency*. Cases **1.** and **2.** reduce to the original GBW model when one of the dipoles is much larger than the other and the model **3.** corresponds to the dipole-dipole cross-section mediated by a two-gluon exchange[11]. For the saturation radius

$$R_0(\Delta\eta) = \frac{1}{Q_0} e^{-\frac{\lambda}{2}(\Delta\eta - \Delta\eta_0)} , \quad (7)$$

we adopt the same set of parameters⁴ as those in [8, 18].

III. DERIVATION

Let us derive the general formulae we get for the cross-sections (1). Defining $u = r_2/r_1$ and $r_{eff}^2 = r_1^2 f_i(u)$, the three scenarios considered in (6) can be rewritten

$$f_1(u) = \frac{u^2}{1+u^2} \quad f_2(u) = \begin{cases} u^2 & \text{if } u < 1 \\ 1 & \text{if } u > 1 \end{cases} \quad f_3(u) = \begin{cases} u^2(1 - \log u) & \text{if } u < 1 \\ 1 + \log u & \text{if } u > 1 \end{cases} . \quad (8)$$

Hence, in the case of g^* -initiated reactions (see Figs.1), formula (1) leads to

$$\frac{\sigma_i}{\sigma_0} = 1 - Q_1 Q_2 \int_0^\infty du \int_0^\infty r dr J_1(r Q_1) J_1(r u Q_2) e^{-\frac{r^2}{4R_0^2} f_i(u)} , \quad (9)$$

which, after integration over r , gives

$$\frac{\sigma_i}{\sigma_0} = 1 - 2R_0^2 Q_1 Q_2 \int_0^\infty \frac{du}{f_i(u)} e^{-(Q_1^2 + Q_2^2 u^2) R_0^2 f_i^{-1}(u)} I_1 \left(\frac{2Q_1 Q_2 u R_0^2}{f_i(u)} \right) , \quad (10)$$

where I_1 is the modified Bessel function of the first kind. Formula (10) gives the theoretical cross-sections within the GBW model for hard hadronic probes.

⁴ One finds[18] $\lambda = .288$ and $\Delta\eta_0 = 8.1$ for $Q_0 \equiv 1 \text{ GeV}$.

Let us discuss it. The factorized dipole distribution $\phi^g(r, Q^2)$ is not positive-definite but this is not *a priori* an obstacle as long as the corresponding total cross-sections(1) stay positive. This is for instance realized by the BFKL cross-section[15] and it will be compulsory to verify whether this positivity is or not altered by saturation. By numerical inspection of formulae (9,10), we checked that the positivity constraint is verified. Qualitatively, this is due to the fact that the negative values of the Bessel functions in (9) are present for large dipole sizes whose contributions are strongly reduced by saturation.

Another constraint is to check that the cross-sections

$$\sigma_{dd} \sim \sigma_0 \frac{r_{\text{eff}}^2}{4R_0^2(\Delta\eta)}, \quad (11)$$

corresponding to the limit of small dipole sizes in (2), lead to cross-sections behaving like $1/\{R_0^2(\Delta\eta) \max(Q_1^2, Q_2^2)\}$, as expected from transparency. Computing the gluon-gluon cross-section in this limit gives

$$\sigma_1 \sim \frac{\sigma_0}{R_0^2} \frac{2Q_1^2 Q_2^2}{(Q_1^2 + Q_2^2)^3} \quad \sigma_2 \sim \frac{\sigma_0}{R_0^2} \delta(Q_1^2 - Q_2^2) \quad \sigma_3 \sim \frac{\sigma_0}{2R_0^2} \min\left(\frac{1}{Q_1^2}, \frac{1}{Q_2^2}\right) \quad (12)$$

which shows that the models **1** and **3** of (6) verify the constraint. The model **2** does not, as confirmed by an explicit integration of (10) which gives in this case

$$\frac{\sigma_2}{\sigma_0} = e^{-R_0^2(Q_1^2 + Q_2^2)} I_0(2R_0^2 Q_1 Q_2) \sim \frac{e^{-R_0^2(Q_1 - Q_2)^2}}{2R_0 \sqrt{\pi} Q_1 Q_2} \rightarrow \frac{\delta(Q_1^2 - Q_2^2)}{R_0^2}, \quad (13)$$

at large R_0 .

It is possible to derive a general formula for saturation in the dipole framework which could be valid for any hard probe expressed in terms of the dipole basis, be it a forward jet, an onium, a virtual photon, etc... In particular, it will be useful to extend the saturation discussion to forward jets at HERA, with a $\gamma^* - g^*$ cross-section. Inserting the Mellin transforms of the dipole distributions

$$\tilde{\phi}(\gamma) = \int d^2r dz (r^2 Q^2)^\gamma \phi(r, z, Q^2), \quad (14)$$

and after some straightforward algebra, we obtain the following inverse Mellin transform expressions:

$$\frac{\sigma_i}{\sigma_0} = \int \frac{d\tau}{2i\pi} \tilde{\phi}^{(1)}(\tau) (2Q_1 R_0)^{-2\tau} \int \frac{d\sigma}{2i\pi} \tilde{\phi}^{(2)}(\sigma) (2Q_2 R_0)^{-2\sigma} g_i(\sigma, \tau); \quad 0 < \text{Re}(\sigma), \text{Re}(\tau), \text{Re}(\sigma + \tau) < 1, \quad (15)$$

where $\tilde{\phi}^{(1)}$ and $\tilde{\phi}^{(2)}$ are the Mellin-transformed dipole distributions in the target and projectile and, for the different models (6), one has

$$\begin{aligned} g_1(\sigma, \tau) &= \frac{\Gamma(1 - \tau - \sigma) \Gamma(\sigma) \Gamma(\tau)}{\Gamma(1 + \tau + \sigma)} \\ g_2(\sigma, \tau) &= \frac{\Gamma(1 - \tau - \sigma)}{\sigma \tau} \\ g_3(\sigma, \tau) &= -2^{-\tau - \sigma} \Gamma(-\tau - \sigma) \{e^{2\sigma} \sigma^{-1 - \tau - \sigma} \Gamma(\tau + \sigma + 1, 2\sigma) + [\tau \iff \sigma]\}. \end{aligned} \quad (16)$$

This formulation allows us to extend easily our computations to various cases, for instance:

$$\tilde{\phi}^g(\tau) = 4^\tau \frac{\Gamma(1 + \tau)}{\Gamma(1 - \tau)} \quad \tilde{\phi}^\gamma(\tau) \propto \pi^{2\tau+1} \frac{\Gamma(1 - \tau) \Gamma(3 - \tau) \Gamma(\tau) \Gamma^2(1 + \tau) \Gamma(2 + \tau)}{\Gamma(4 - 2\tau) \Gamma(2 + 2\tau)}, \quad (17)$$

which are easily obtained from the corresponding *impact factors*. After easy transformations, one gets for the different GBW models

$$\begin{aligned} \frac{\sigma_1}{\sigma_0} &= \int_0^\infty dx J_1(x) A^{(1)}(x Q_1 R_0) A^{(2)}(x Q_2 R_0); \quad A(x) = \int \frac{d\tau}{2i\pi} x^{-2\tau} \tilde{\phi}(\tau) \Gamma(\tau) \\ \frac{\sigma_2}{\sigma_0} &= \int_0^\infty 2x dx e^{-x^2} B^{(1)}(2x Q_1 R_0) B^{(2)}(2x Q_2 R_0); \quad B(x) = \int \frac{d\tau}{2i\pi} x^{-2\tau} \frac{\tilde{\phi}(\tau)}{\tau} \\ \frac{\sigma_3}{\sigma_0} &= \frac{\sigma_2}{\sigma_0} + \int_0^\infty 2x dx e^{-x^2} \left(C^{(1)}(2x Q_1 R_0) D^{(2)}(2Q_2 R_0, x) + D^{(1)}(2Q_1 R_0, x) C^{(2)}(2x Q_2 R_0) \right) \end{aligned} \quad (18)$$

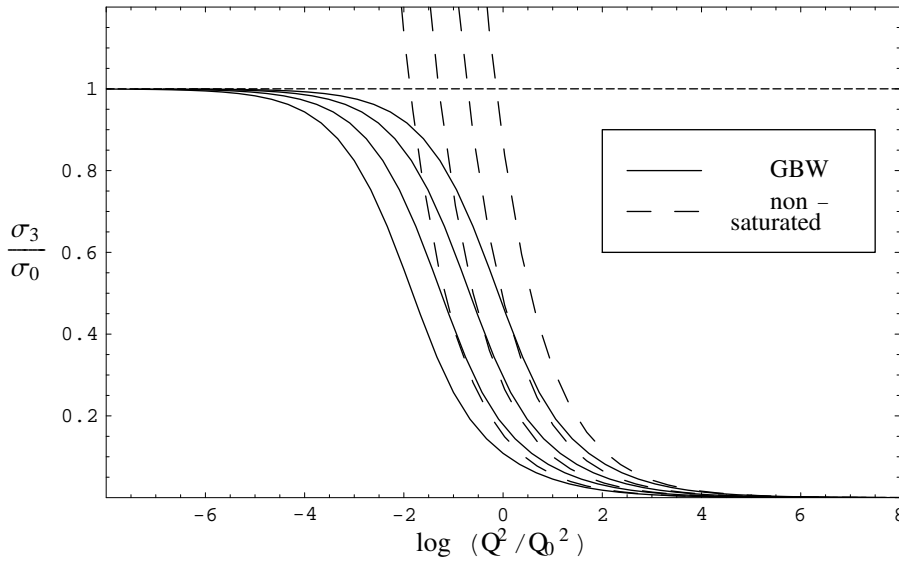


FIG. 2: $g^* - g^*$ cross-sections (model **3**). $Q_1 = Q_2 = Q$: symmetric virtuality case. $\Delta\eta =$ (from left to right) 4, 6, 8, 10 : rapidity intervals. Full lines: saturation cross-sections (10). Dashed lines: without saturation (12).

where

$$C(x) = \int \frac{d\tau}{2i\pi} x^{-2\tau} \tilde{\phi}(\tau) ; \quad D(Q, x) = \int \frac{d\tau}{2i\pi} (Qx)^{-2\tau} \frac{\tilde{\phi}(\tau)}{\tau(2\tau + x^2)} . \quad (19)$$

With these general formulae, we find back our previous results (9,10,13) for g^* and obtain⁵ those for γ^* .

IV. APPLICATION

Let us investigate the phenomenological outcome, for hadron colliders, of our extension of the GBW models to hadronic (*i.e.* g^*) probes. The theoretical cross-sections are obtained from formulae (8)-(10) and (15)-(19), in terms of the physical variables Q_1, Q_2 and $\Delta\eta$, once the saturation scale parameters Q_0, λ and $\Delta\eta_0$ are taken identical to their reference values (see footnote 4).

In Fig.2, we display the cross-section ratio σ_3/σ_0 as a function of $\log(Q^2/Q_0^2)$, where $Q = Q_1 = Q_2$ for values of the rapidity interval $\Delta\eta = 4, 6, 8, 10$. We also compare with the corresponding ratio for the non-saturated case (12). As expected, the curves show the well-known trend of the GBW model, namely a suppression of the non-saturated cross-section, with a convergence towards the full saturation limit $\sigma \rightarrow \sigma_0$. In order to appreciate more quantitatively the influence of saturation, it is most convenient to consider the quantities $\mathcal{R}_{i/j}$ defined as

$$\mathcal{R}_{i/j} \equiv \frac{\sigma(Q_1, Q_2, \Delta\eta_i)}{\sigma(Q_1, Q_2, \Delta\eta_j)} , \quad (20)$$

i.e. the cross-sections ratios for two different values of the rapidity interval. These ratios display in a clear way the saturation effects. They also correspond to possible experimental observables since they can be obtained from measurements at fixed values of the virtual gluon light-cone momentum and thus are independent of the gluon structure functions of the incident hadrons. Indeed, such observables have been used for a study of Mueller-Navelet jets for testing BFKL predictions at the Tevatron[20, 21, 22].

⁵ Note that the input functions A, B, C, D (18,19) correspond to specific Meijer functions[19].

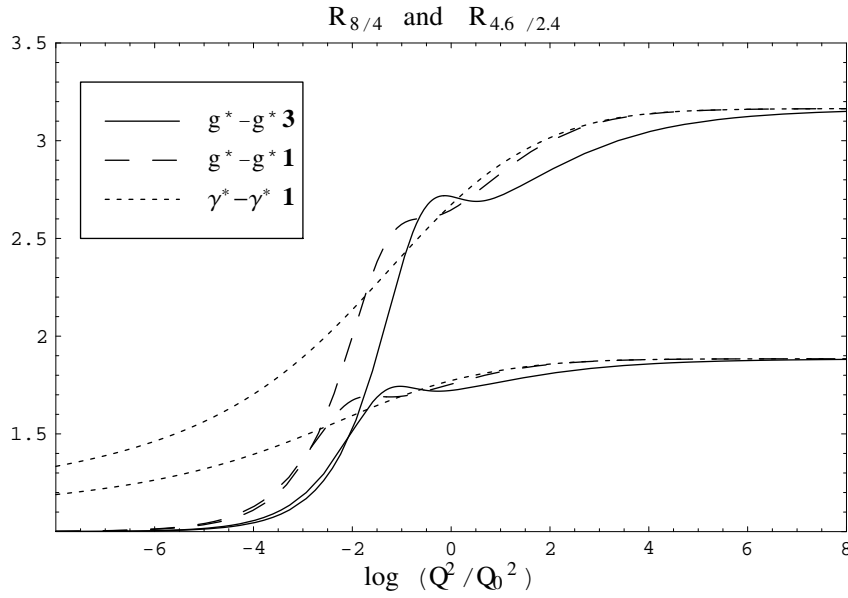


FIG. 3: *Cross-section ratios* $\mathcal{R}_{i/j}$. The resulting ratios for models **1** and **3** are plotted for rapidity intervals $i = 8, j = 4$ and $i = 4.6, j = 2.4$. The comparison is made with $\gamma^*-\gamma^*$ ratios for model **1** and equivalent kinematics. The non-saturated case would be a constant corresponding to the high Q^2 limit of the plots.

In Fig.3 we plot the values of $\mathcal{R}_{4.6/2.4}$ (resp. $\mathcal{R}_{8/4}$) as a function of $Q_1 = Q_2 \equiv Q$. These ratios correspond to values for Mueller-Navelet jets studied at the Tevatron[20, 21] (resp. realistic for the LHC[22]). The results are displayed both for models **1** and **3**, see (6).

As expected from the larger rapidity range, the decrease of \mathcal{R} between the transparency regime and the saturated one is larger for the LHC than for the Tevatron. The striking feature of Fig.3 is that the effect of saturation appears as a sharp transition for some critical range in Q (higher for the LHC).

Let us compare the resulting ratios for hadronic probes (g^* -initiated) to those for the virtual photon (γ^* -initiated) for the same values of the rapidity ranges, see Fig.3. Interestingly enough, the photon transition curve is much smoother, a phenomenon which can be explained by the different structure of the dipole distribution function. Indeed, as discussed previously[15], the g^* dipole distribution has a tail extended towards large dipole sizes, which are more damped by the saturation corrections. Hence the gluon dipole distribution is more abruptly cut by saturation effects than the photon one.

In Fig.4, we display the variation of $\mathcal{R}_{8/4}$, when one looks for asymmetric situations, *i.e.* $Q_1 > Q_2$. As seen from the figure, the transition may become even sharper in this case, with the formation of a bump at a rather high value of Q_1 , which could provide an interesting signal for the saturation scale. Indeed, the origin of this bump lies in the different rate of increase of the cross-sections towards saturation when the virtualities are different enough. This possible signal is present at rather high scale, which could be useful for experimental considerations, as we shall develop now.

i) Mueller-Navelet jets

Two jets separated by a large rapidity interval, or Mueller-Navelet jets[23], are the more natural process for our formulae (9,10) to be applied. Indeed, a measurement of those dijet cross-sections has been performed at Tevatron, with jets of transverse momentum with a lower E_T cut. To actually measure the ratio \mathcal{R} in order to get rid of uncertainties on the structure functions, the two available incident energies (630 GeV and 1800 GeV) were used. The result was a strong increase of \mathcal{R} (integrated over E_T) with the rapidity interval, which was pointed out as a possible hint of BFKL evolution. However, the BFKL evolution at Tevatron energies appears to be quite sizeably modified by finite energy and running coupling corrections[24]. Saturation studies are favored by large rapidity intervals (as demonstrated in Fig.(3)). The relevant range of virtuality Q for expecting a clear saturation signal is albeit rather low (see Fig.3,4).

If the strong experimental signal reported in [20] appears to be confirmed, the saturation prediction displayed in Fig.3 could well be relevant (with a redefinition of the parameters). Anyway, a simulation of Mueller-Navelet jets that would incorporate the relation between the E_T of the jet and the virtuality Q of the probing g^* is needed to discuss the feasibility of saturation tests.

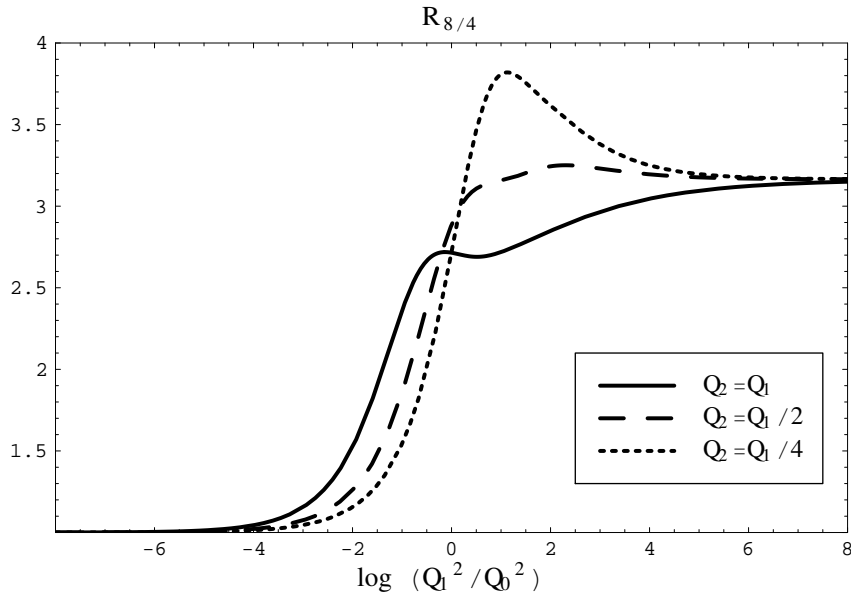


FIG. 4: $\mathcal{R}_{8/4}$, *asymmetric case*. The curves are drawn for model **3**. Note the bump at $Q_1^2/Q_0^2 \sim 3$.

ii) Heavy vector mesons

As an alternative to hard forward jets, one could figure out[25] the detection of two heavy vector mesons with moderate transverse momentum and separated by large rapidity intervals. Indeed, using J/Ψ 's or Υ 's may provide a hadronic probe of precise mass and transverse momentum. It potentially realizes a $q\bar{q}$ probe and thus could give an information on the differential distribution of dipoles ϕ^g , for instance on the dipole size distribution. Moreover, its leptonic decays may facilitate the event selection.

iii) Charmed and beauty hadrons

A forward jet detection corresponds to one of the $q\bar{q}$ partners of a dipole. The detection of a heavy flavor meson would give a similar interesting signal. One thus would look for the detection of heavy flavored mesons separated by a large rapidity interval. In particular, the detection of a D^* on one side and a B -meson on the other side would realize interesting asymmetric configurations such as seen on Fig.4. One could also play with their transverse momentum to vary the g^* virtualities.

These possibilities of realizing hadronic probes of saturation certainly deserve more studies in the near future. Simulation of these processes at Tevatron and LHC energies will give a quantitative estimate of the potential of hadronic colliders to reveal new features of saturation.

V. CONCLUSION AND OUTLOOK

Let us briefly summarize the main results of our study.

We started from an extension of the Golec-Biernat and Wüsthoff saturation model to hadronic collisions. For this sake, we use a QCD dipole formulation[15, 16] of hard hadronic probes based on a k_T -factorization assumption; such probes as forward (Mueller-Navelet) jets, heavy mesons, heavy flavoured mesons are initiated by off-mass-shell gluons. Our results are:

- i) A derivation of saturation predictions for total hard cross-sections at hadron colliders, *e.g.* the Tevatron and LHC.
- ii) Observables which possess a potentially clear signal for saturation at high rapidity intervals and gluon virtualities around the expected saturation scale in dipole-dipole interactions, see Figs(2-4).
- iii) The suggestion of using, besides the well-known Mueller-Navelet jets, heavy vector and/or heavy flavored mesons to measure hard cross-sections and their transition towards saturation.

There are quite a few open issues for the present formalism:

On a phenomenological ground, it indicates a way for simulations in the framework of hadron colliders using the QCD dipole formalism which had been so useful in the HERA context. These phenomenological studies will tell us

whether and how saturation could be present and checked at the Tevatron and/or the LHC. Note also that forward jets at HERA, which are initiated by $g^* - \gamma^*$ configurations with large rapidity separation, could be interesting to investigate. Beyond the scope of the present paper, determinant experimental issues, like fighting against pile-up events, background studies, possibility of a direct access to the hard cross-section ratios $\mathcal{R}_{i/j}$, etc... deserve to be explored.

On the theoretical ground, a study going beyond the single $q\bar{q}$ basis for the hard probe dipole distribution is deserved. In particular, adding the $gq\bar{q}$ or few-dipole configurations is important to discuss the k_T -factorization assumption. It may also allow us to extend our formalism to diffraction processes, since such configurations appeared important for the GBW model[8] at HERA. It is also possible to extend the saturation analysis beyond the GBW formulation and to directly introduce solutions[26] of the non-linear QCD evolution equations, which would have a natural BFKL (and not only transparency) limit at low density.

Acknowledgments

We thank Christophe Royon and Stéphane Munier for useful comments and suggestions.

-
- [1] L. N. Lipatov, *Sov. J. Nucl. Phys.* **23**, (1976) 338; E. A. Kuraev, L. N. Lipatov, and V. S. Fadin, *Sov. Phys. JETP* **45**, (1977) 199; I. I. Balitsky and L. N. Lipatov, *Sov. J. Nucl. Phys.* **28**, (1978) 822.
 - [2] L. V. Gribov, E. M. Levin, and M. G. Ryskin, *Phys. Rep.* **100**, (1983) 1.
 - [3] A. H. Mueller and J. Qiu, *Nucl. Phys.* **B268**, (1986) 427.
 - [4] L. McLerran and R. Venugopalan, *Phys. Rev.* **D49**, (1994) 2233; *ibid.*, (1994) 3352; *ibid.*, **D50**, (1994) 2225; A. Kovner, L. McLerran, and H. Weigert, *Phys. Rev.* **D52**, (1995) 6231; *ibid.*, (1995) 3809; R. Venugopalan, *Acta Phys.Polon.* **B30**, (1999) 3731; E. Iancu, A. Leonidov, and L. McLerran, *Nucl. Phys.* **A692**, (2001) 583; *Phys. Lett.* **B510**, (2001) 133; E. Iancu and L. McLerran, *Phys. Lett.* **B510**, (2001) 145; E. Ferreiro, E. Iancu, A. Leonidov, and L. McLerran, *Nucl. Phys.* **A703**, (2002) 489; H. Weigert, *Nucl. Phys.* **A703**, (2002) 823.
 - [5] I. Balitsky, *Nucl. Phys.* **B463**, (1996) 99; Y. V. Kovchegov, *Phys. Rev.* **D60**, (1999) 034008; *ibid.*, **D61**, (2000) 074018.
 - [6] E. Levin and J. Bartels, *Nucl. Phys.* **B387**, (1992) 617; Y. V. Kovchegov, *Phys. Rev.* **D61**, (2000) 074018; E. Levin and K. Tuchin, *Nucl. Phys.* **A693**, (2001) 787; *ibid.*, **A691**, (2001) 779.
 - [7] A. H. Mueller and D. N. Triantafyllopoulos, *Nucl. Phys.* **B640**, (2002) 331.
 - [8] K. Golec-Biernat and M. Wüsthoff, *Phys. Rev.* **D59** (1998) 014017, *Phys. Rev.* **D60** (1999) 114023.
 - [9] G. Altarelli and G. Parisi, *Nucl. Phys.* **B126** 18C (1977) 298. V. N. Gribov and L. N. Lipatov, *Sov. Journ. Nucl. Phys.* (1972) 438 and 675. Yu. L. Dokshitzer, *Sov. Phys. JETP.* **46** (1977) 641. For a review: Yu. L. Dokshitzer, V. A. Khoze, A. H. Mueller, and S. I. Troyan *Basics of perturbative QCD* (Editions Frontières, J. Tran Thanh Van Ed. 1991).
 - [10] N. N. Nikolaev and B. G. Zakharov, *Zeit. für. Phys.* **C49** (1991) 607; *Phys. Lett.* **B332** (1994) 184.
 - [11] A. H. Mueller, *Nucl. Phys.* **B415** (1994) 373; A. H. Mueller and B. Patel, *Nucl. Phys.* **B425** (1994) 471; A. H. Mueller, *Nucl. Phys.* **B437** (1995) 107.
 - [12] S. Catani, M. Ciafaloni, and F. Hautmann, *Nucl. Phys.* **B366** (1991) 135. J. C. Collins and R. K. Ellis, *Nucl. Phys.* **B360** (1991) 3; E. M. Levin, M. G. Ryskin, Yu. M. Shabelsky, and A. G. Shuvaev, *Sov.J.Nucl.Phys.* **53** (1991) 657.
 - [13] S. Munier, R. Peschanski, *Nucl. Phys.* **B524** (1998) 377. A. Bialas, H. Navelet, R. Peschanski, *Nucl. Phys.* **B593** (2001) 438.
 - [14] J. D. Bjorken, J. Kogut, and Soper, *Phys.Rev.* **D3** (1971) 1382.
 - [15] R. Peschanski, *Mod.Phys.Lett.* **A15** (2000) 1891.
 - [16] S. Munier, *Phys.Rev.* **D63** (2001) 034015.
 - [17] F. Gelis and R. Venugopalan, *Large mass Q-Qbar production from the Color Glass Condensate*, hep-ph/0310090.
 - [18] N. Timneanu, J. Kwieciński, and L. Motyka, *Eur.Phys.J.* **C23** (2002) 513, *Acta Phys.Polon.* **B33** (2002) 1559 and 3045.
 - [19] A. Prudnikov, Y. Brychkov, and O. Marichev, *Integrals and Series* (Gordon and Breach Science Publishers, 1986).
 - [20] A. Goussiou, for the D0 collaboration, *Dijet Cross section at large s/Q^2 in pp Collisions*, presented at the ‘International Europhysics Conference On High-Energy Physics’ (EPS-HEP 99), Tampere, Finland, July, 1999.
 - [21] J. G. Contreras, R. Peschanski, and C. Royon, *Phys.Rev.* **D62** (2000) 034006.
 - [22] R. Peschanski and C. Royon, *Pomeron intercepts at colliders*, Workshop on physics at LHC, hep-ph/0002057.
 - [23] A. H. Mueller and H. Navelet, *Nucl.Phys.* **B282** (1987) 727.
 - [24] L. H. Orr and W. J. Stirling, *Phys. Lett.* **B429** (1998) 135.
 - [25] C. Royon, private communication.
 - [26] E. Iancu, K. Itakura, and S. Munier, *Saturation and BFKL dynamics in the HERA data at small x*, hep-ph/0310338.